

# Isothermal Martensitic Transformation in Fe-Ni-Cr Alloy

著者	IMAI Yunoshin, IZUMIYAMA Masao, SASAKI Kyo
journal or publication title	Science reports of the Research Institutes, Tohoku University. Ser. A, Physics, chemistry and metallurgy
volume	17/18
page range	39b-48b
year	1965
URL	<a href="http://hdl.handle.net/10097/27275">http://hdl.handle.net/10097/27275</a>

# Isothermal Martensitic Transformation in Fe-Ni-Cr Alloy\*

Yûnoshin IMAI, Masao IZUMIYAMA and Kyô SASAKI

*The Research Institute for Iron, Steel and Other Metals*

(Received March 10, 1966)

## Synopsis

The spontaneous martensitic transformations were investigated by using the Fe-base alloy containing 17 per cent Cr and 8 per cent Ni. The isothermal martensitic transformations occurred while it was held at above the  $M_s^{\gamma \rightarrow \alpha'}$  temperature and the T.T.T. diagram was of the form with two noses at about  $-100^\circ$  and  $-135^\circ\text{C}$ , respectively. According to X-ray analysis h.c.p. structure ( $\epsilon$ ) was formed at the upper nose. The driving force ( $\Delta F^{\gamma \rightarrow \epsilon}$ ) of transformation in this alloy was 22 cal/mol. This value was derived from an assumption in which the transformation would occur owing to a very low stacking fault energy. Furthermore, from this assumption, it was suggested that the  $\gamma \rightarrow \epsilon$  transformation would occur at above 7 per cent Ni content. This suggestion agreed closely with practical data. The b.c.c. martensite ( $\alpha'$ ) grew when it was held longer in the temperature range of the upper nose. The habit plane of this  $\alpha'$  was  $(111)_\gamma$  plane, whereas the habit plane of the  $\alpha'$  formed isothermally in the temperature range of the lower nose and athermally at a temperature below  $M_s^{\gamma \rightarrow \alpha'}$  was  $(225)_\gamma$  plane.

## I. Introduction

In the previous works<sup>(1)-(4)</sup>, it was shown that h.c.p. product of martensitic structure ( $\epsilon$ ) was formed with b.c.c. product ( $\alpha'$ ) in 18 per cent Cr-8 per cent Ni stainless steel by cold-working at subatmospheric temperature or by subatmospheric cooling only.

In a previous paper<sup>(5)</sup>, the thermodynamic properties of athermal and isothermal martensitic transformation in Fe-Ni-Cr and Fe-Ni-Mn system were shown. The present paper describes the results of morphologic and crystallographic studies of martensite formed isothermally and the conditions of isothermal martensitic transformation.

## II. Experiments

The chemical composition of the specimens used was as follows: C 0.11%, Si

- 
- \* The 1230th report of the Research Institute for Iron, Steel and Other Metals. Reported in Japanese in the J. Japan Inst. Met., **27** (1963), 513.
- (1) H.C. Fiedler, B.L. Averbach and M. Cohen, Trans. ASM, **47** (1955), 267.
  - (2) H. Otte, Acta Met., **5** (1957), 614.
  - (3) R.P. Reed, Acta Met., **10** (1962), 865.
  - (4) J.F. Beedis and W.D. Robertson, Acta Met., **10** (1962), 1077.
  - (5) Y. Imai and M. Izumiyama, Nippon Kinzoku Gakkai-Si, **27** (1963), 170. Also Sci. Rep. RITU, **A 17** (1965), 135.

0.29%, Mn 0.44%, Cr 16.93% and Ni 8.18%. The amount of isothermal martensite transformation was determined by measuring the electrical resistance. The specimens, 1 mm in diameter and 100 mm in length, were held for 1 hr at 1100°C in vacuum of  $10^{-5}$  mmHg, quenched in water and then, electrolytically polished (removing about 0.02 mm) prior to measuring the electrical resistance.

### III. Results and discussion

Fig. 1 shows the changes in electrical resistance due to isothermal martensitic transformation while the specimens were held at various temperatures. Fig. 2 shows a diagram of isothermal martensitic transformation derived from Fig. 1. The diagram shows the curves with two noses at about  $-100^{\circ}\text{C}$  and  $-135^{\circ}\text{C}$  respectively above  $M_s^{\gamma \rightarrow \alpha'}$  temperature. From this diagram, two kinds of reactions are suggested, because it has been known that isothermal martensitic transforma-

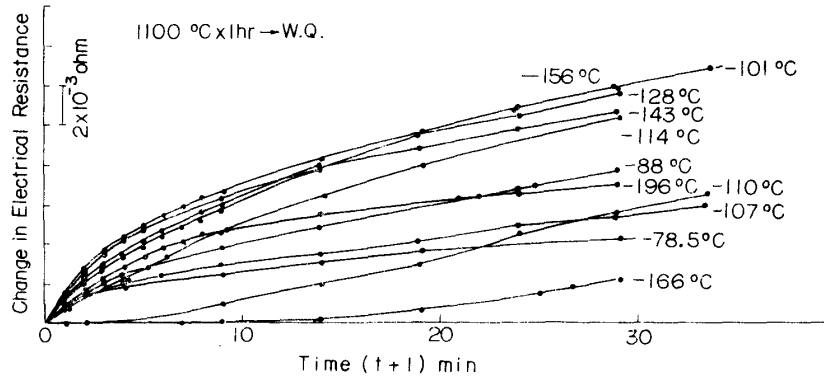


Fig. 1. Changes in electrical resistance due to isothermal martensitic transformation at various temperatures.

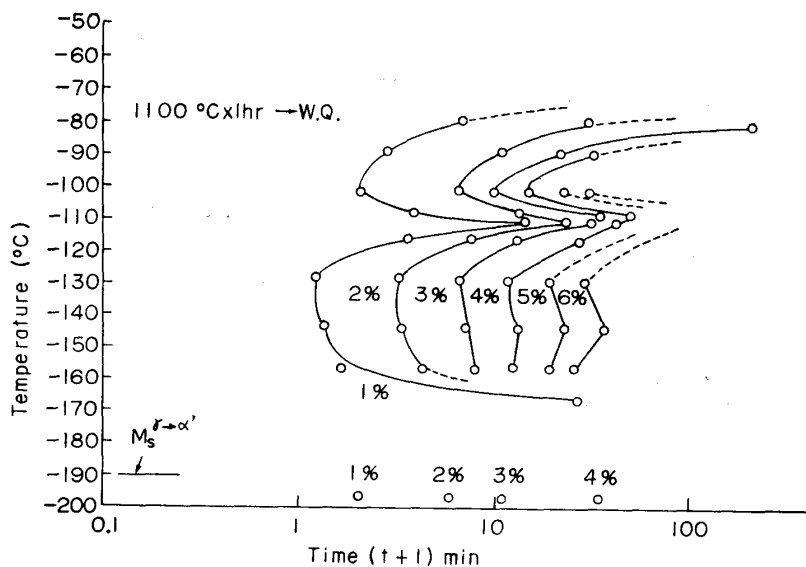
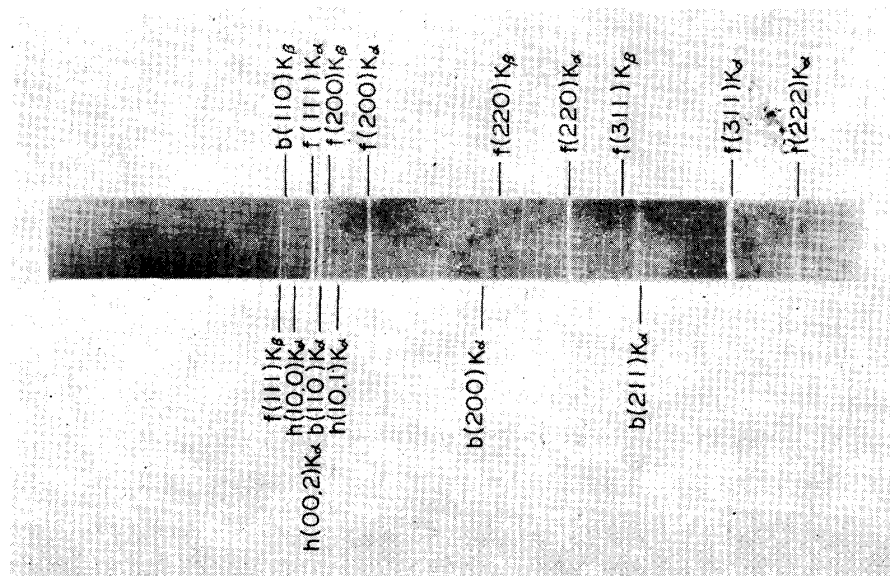


Fig. 2. Transformation-temperature-time curves showing progress of isothermal martensitic transformation.



Phot. 1. X-ray diffraction pattern in 17 per cent Cr-8 per cent Ni-Fe alloy treated isothermally at  $-100^{\circ}\text{C}$  for 1hr. Fe- $K\alpha$  radiation.

Table 1. Powder lines of 17 per cent Cr-8 per cent Ni-Fe alloy analyzed from Phot. 1.

No.	sin $\theta$	hkl			I
		f. c. c.	b. c. c.	h. c. p.	
1	0.4308	(111) $K\beta$			w
2	0.4415		(110) $K\beta$		w
3	0.4472			(10.0) $K\alpha$	v w
4	0.4729	(111) $K\alpha$			v s
5	0.4823		(110) $K\alpha$	(00.2) $K\alpha$	s
6	0.4942	(200) $K\beta$			w
7	0.5065			(10.1) $K\alpha$	w
8	0.5446	(200) $K\alpha$			s
9	0.6780		(200) $K\alpha$		w
10	0.6955	(220) $K\beta$			w
11	0.7660	(220) $K\alpha$			s
12	0.8136	(311) $K\beta$			w
13	0.8281		(211) $K\alpha$		m
14	0.8963	(311) $K\alpha$			v s
15	0.9351	(222) $K\alpha$			s

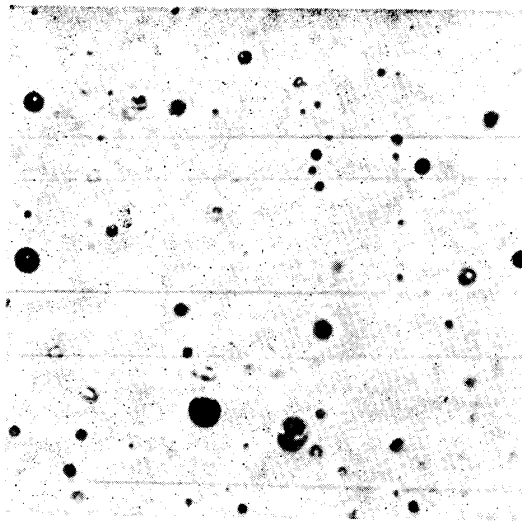
Table 2. Lattice parameters of various phases formed in 17 per cent Cr-8 per cent Ni-Fe alloy.

f. c. c.	$a=3.588\text{\AA}$
b. c. c.	$a=2.860\text{\AA}$
h. c. p.	$a=2.499\text{\AA}$
	$c=4.080\text{\AA}$
	$c/a=1.633$

tion curves show C-type with a single nose<sup>(6)</sup>. X-ray analysis was carried out at room temperature on the specimen held at  $-100^{\circ}\text{C}$ , that is, at upper nose, in order to clarify the two reactions. Phot. 1 shows the X-ray diffraction patterns of the specimen treated isothermally at  $-100^{\circ}\text{C}$  for 1 hour. Tables 1 and 2 show the results of analysis of Phot. 1. As shown in Table 1, the diffraction lines of h.c.p. product ( $\epsilon$ ) are seen together with those of f.c.c. ( $\gamma$ ) and of b.c.c. ( $\alpha$ ) structures. The lattice parameters of these three phases are shown in Table 2.

From the above-mentioned results, it was shown that the  $\gamma \rightarrow \epsilon$  transformation would occur isothermally at the temperature of the upper nose without additional deformation.

Phot. 2 shows the surface relief due to the  $\gamma \rightarrow \epsilon$  transformation, as is conceivable from the previous works<sup>(7)</sup>. The habit plane of  $\epsilon$  phase is parallel to the  $(111)_{\gamma}$  plane. Photos. 3 and 4 show the transmission electron microscopic structures. Some workers have been reported that the  $\epsilon$  phase is of the needle-like or of the plate-let structure. But it can be seen in Phot. 4 that the form of  $\epsilon$  phase is plate-let rather than needle-like.



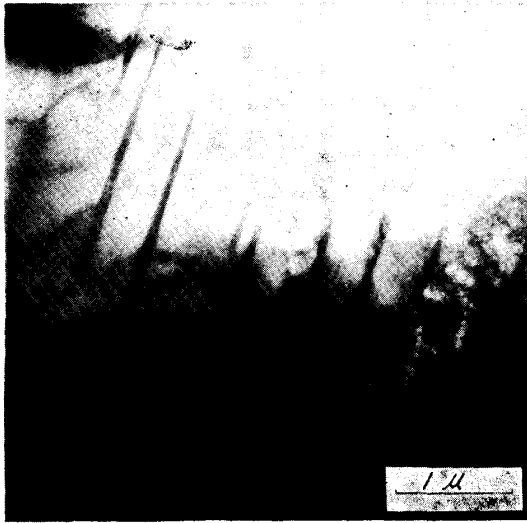
Phot. 2. Surface relief due to  $\gamma \rightarrow \epsilon$  isothermal transformation at  $-100^{\circ}\text{C}$ . ( $\times 480$ )

The thermodynamic properties of the  $\gamma \rightleftharpoons \alpha'$  transformation were analyzed by using the relation of equilibrium between  $\gamma$  and  $\alpha$  phases in the previous report<sup>(5)</sup>. However, in the case of the  $\gamma \rightleftharpoons \epsilon$  transformation, the thermodynamic properties cannot be derived from a similar equilibrium relation, because there is no  $\epsilon$  phase in pure iron. Therefore, the free energy change accompanying the  $\gamma \rightleftharpoons \epsilon$  transformation was derived from an assumption as follows: In the previous work<sup>(8)</sup>, it is proposed as mechanism of the f.c.c.  $\rightarrow$  h.c.p. transformation that the  $(111)_{\gamma}$  plane converts into the  $(0001)_{\epsilon}$  and every second  $(111)_{\gamma}$  plane is displaced by a distance  $a/6$  in the

(6) R.E. Cech and J.H. Hollomon, *Trans. AIME*, **197** (1953), 685.

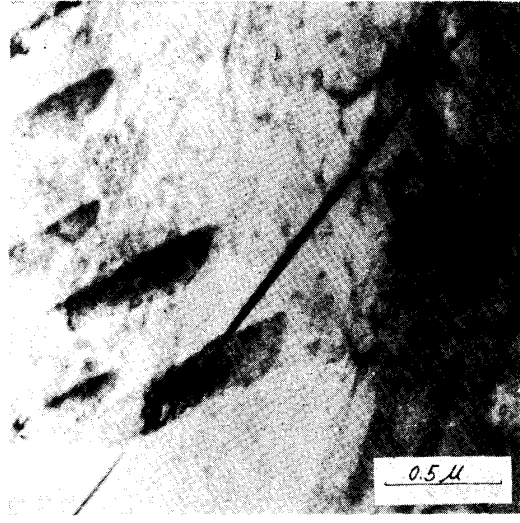
(7) J.A. Venable, *Phil. Mag.*, **7** (1962), 35.

(8) J.W. Christian, *Proc. Roy. Soc.*, **A 206** (1951), 51.



Phot. 3.

Phot. 3. Transmission electron microscopic structure of 17 per cent Cr-8 per cent Ni-Fe alloy. Needle-like structure represents  $\epsilon$ .



Phot. 4.

Phot. 4. Transmission microscopic structure of 17 per cent Cr-8 per cent Ni-Fe alloy. Needle-like and plate-let structures represent  $\epsilon$ .

$[112]_{\gamma}$  direction, where  $a$  is the lattice parameter of the  $\gamma$  phase. That is, the h.c.p. phase will be formed when the perfect dislocations on the slip plane of the  $\gamma$  phase split into Heidenreich and Schockley's two half-dislocations ( $a/2[10\bar{1}] \rightarrow a/6[11\bar{2}] + a/6[2\bar{1}\bar{1}]$ ) and when either of the two half-dislocations rotates around a pole-dislocation having Burger's vector, of which the perpendicular component to a slip plane is the distance of two atomic planes. Therefore, the condition of transformation may be written as follows:

$$E = \sigma_{\epsilon} b_{\epsilon}, \quad (1)$$

where  $E$  is the energy of the stacking fault,  $\sigma_{\epsilon}$  is the force necessary to initiate the transformation of the f.c.c. phase into the h.c.p. phase and  $b_{\epsilon}$  is the component in  $\langle 112 \rangle_{\gamma}$  direction of Burger's vector. According to the previous work<sup>(9)</sup>, the stacking fault energy of 18 per cent Cr-8 per cent Ni stainless steel was quite small, being about 13 erg/cm<sup>2</sup>. As  $b_{\epsilon}$  is  $a/\sqrt{6}$ ,  $a$  being  $3.588 \times 10^{-8}$  cm,  $\sigma_{\epsilon}$  becomes  $8.91 \times 10^8$  dyne/cm<sup>2</sup>  $\approx 9$  kg/mm<sup>2</sup>. In practical isothermal transformation of  $\gamma$  into  $\epsilon$  phase, the difference in chemical free energy between  $\gamma$  and  $\epsilon$  phases, namely,  $\Delta F_{\gamma \rightarrow \epsilon}$  instead of  $\sigma_{\epsilon}$  will play a role of driving force. It has been shown that the relation between  $\Delta F_{\gamma \rightarrow \epsilon}$  and the resistance to deformation,  $f$ , can be expressed as follows:

$$\Delta F_{\gamma \rightarrow \epsilon} = f \cdot \Delta L^{(10)}, \quad (2)$$

where  $\Delta L$  is the amount of shear strain caused by the transformation. If it is assumed that the transformation occurs when  $\sigma_{\epsilon} = f$ , combining Eqs. (1) and (2),

(9) M.J. Whelan, Proc. Roy. Soc. A **249** (1959), 114.

(10) S. Takeuchi and H. Suzuki, Nippon Kinzoku Gakkai-Si, **13** (1946), No. 1, 26; **B 14** (1950), No. 2, 12.

the difference in free energy between  $\gamma$  and  $\varepsilon$  phases will be

$$\Delta F_{\gamma \rightarrow \varepsilon} = \sigma_{\varepsilon} \cdot \Delta L. \quad (3)$$

If the transformation of  $\gamma$  into  $\varepsilon$  phase satisfies the Shoji-Nishiyama relationship  $(111)_{\gamma} // (0001)_{\varepsilon}$  and  $[11\bar{2}]_{\gamma} // [1\bar{1}00]_{\varepsilon}$ ,  $\Delta L$  can be obtained from the amount of deformation component in the shear direction, which is 0.144. Taking this value as  $\Delta L$  and taking  $\sigma_{\varepsilon}$  in Eq. (1) to be about  $8.91 \times 10^8$  dyne/cm<sup>2</sup>, the difference in free energy between  $\gamma$  and  $\varepsilon$  phases will become

$$\Delta F_{\gamma \rightarrow \varepsilon} = 1.28 \times 10^8 \text{ dyne/cm}^2 = 22 \text{ cal/mol.}$$

The condition of transformation shown in Eq. (1) will be reconsidered from another point of view before an examination of its thermodynamic properties. It has been known that the martensitic transformation can be formally considered as a kind of mechanical deformation<sup>(10)</sup>. When external force  $\sigma$  exceeds the elastic limit, the relation between  $\sigma$  and strain  $S$  can be expressed as follows:

$$\sigma = d\sigma/dS \cdot S \quad (4)$$

Using an assumption that the shear direction due to the martensitic transformation agrees with the slip direction, the value of  $S$  is 0.144 equal to  $\Delta L$  in Eq. (3). And  $d\sigma/dS$  can be derived from Fig. 3<sup>(11)</sup>. That is,  $d\sigma/dS$  is given by tangent at  $S=0.144$  in this figure, being 62 kg/mm<sup>2</sup>. Using these values,  $\sigma$  in Eq. (4) becomes  $8.9 \times 10^8$  dyne/cm<sup>2</sup>  $\approx 9$  kg/mm<sup>2</sup>, which agrees well with  $\sigma_{\varepsilon}$  (9 kg/mm<sup>2</sup>) in Eq. (1). Therefore, it seems that the assumption in Eq. (1) is appropriate. The stress-strain curve in Fig. 3 is not the true one, but the difference between the true and the nominal stress-strain curve is negligibly small provided the strain is small, such as f.c.c.  $\rightarrow$  h.c.p. transformation. Accordingly, the thermodynamic properties of f.c.c.  $\rightarrow$  h.c.p.

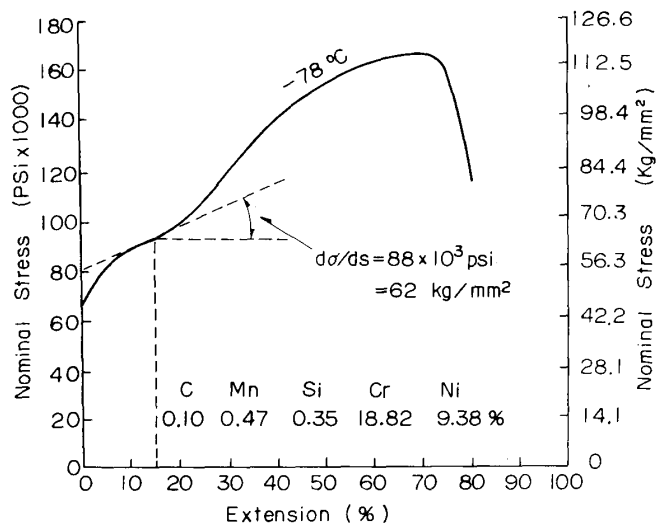


Fig. 3. Variation of nominal stress with extension, annealed 18-8 Cr-Ni steel. (After D.J. McAdam, G.W. Geil and F.J. Cromwell)

(11) D.J. McAdam, G.W. Geil and F.J. Cromwell, *Trans. ASM*, **41** (1949), 609.

transformation was investigated assuming the condition of transformation shown in Eq. (1). Generally, the temperature  $T_0$  at which  $-\Delta F_{\gamma \rightarrow \epsilon} = 0$  is given by  $(M_s + A_s)/2$ , where  $A_s$  is austenite start temperature on heating. According to Reed,<sup>(3)</sup>  $A_s^{\epsilon \rightarrow \gamma}$  of 18 per cent Cr-8 per cent Ni stainless steel is about 413°K. On the other hand,  $M_s^{\gamma \rightarrow \epsilon}$  can be obtained from Fig. 2, which is about 203°K. Accordingly,  $T_0^{\gamma \rightarrow \epsilon}$  becomes about 308°K. Fig. 4 shows the relation between the free energy change accompanying the martensitic transformation in Fe-Ni-Cr system and the temperature. As the free energy change accompanying the  $\gamma \rightarrow \alpha'$  transformation has been previously reported<sup>(5)</sup>, in the present case only the free energy change due to the martensitic transformation of 17 per cent Cr-8 per cent Ni-Fe alloy will be described, which is indicated by the marks A, B and C in Fig. 4.  $T_0^{\gamma \rightarrow \alpha'}$  of this alloy is 760°K. The  $\gamma \rightarrow \alpha'$  transformation will not occur until  $\gamma$  phase is supercooled to the point B, because the stored free energy must overcome the strain energy due to the martensitic transformation. On the other hand, in the case of f.c.c.  $\rightarrow$  h.c.p. transformation,  $T_0^{\gamma \rightarrow \epsilon}$  is lower than  $T_0^{\gamma \rightarrow \alpha'}$  and it seems that the strain energy induced by f.c.c.  $\rightarrow$  h.c.p. transformation is smaller than that of  $\gamma \rightarrow \alpha'$  transformation. Accordingly, the degree of supercooling of the f.c.c.  $\rightarrow$  h.c.p. transformation is smaller than that of  $\gamma \rightarrow \alpha'$  transformation, and the f.c.c.  $\rightarrow$  h.c.p. transformation occurs at the temperature E. That is, as shown in Fig. 4 and Eq. (3), the driving force necessary to initiate  $\gamma \rightarrow \alpha'$  transformation is 520 cal/mol at  $M_s^{\gamma \rightarrow \alpha'}$  temperature, but in the case of the f.c.c.  $\rightarrow$  h.c.p. transformation this is not larger than 22 cal/mol.

In Fig. 4,  $M_s^{\gamma \rightarrow \alpha'}$  point changes along the curve BHI with the increase in Ni content from 3 to 10 per cent maintaining 17 per cent Cr. On the other hand, it is suggested that in the case of the f.c.c.  $\rightarrow$  h.c.p. transformation,  $M_s^{\gamma \rightarrow \epsilon}$  point does not

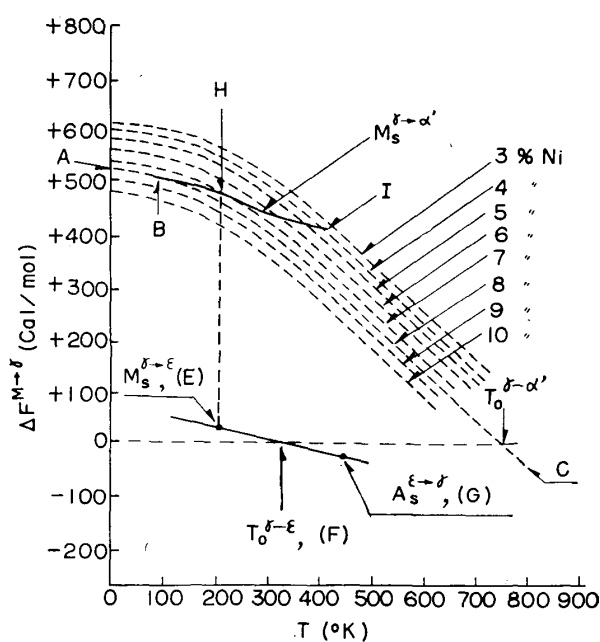
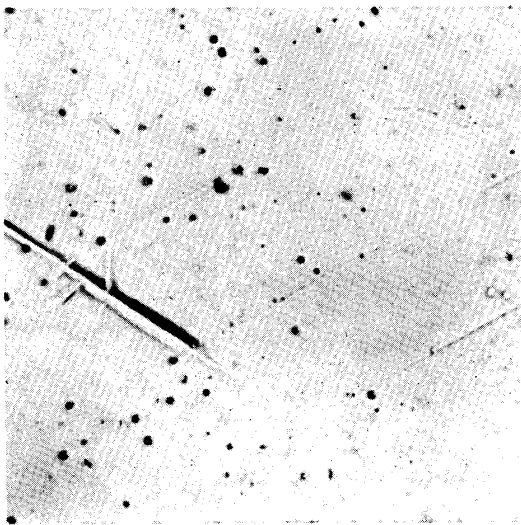


Fig. 4. The free energy changes accompanying martensitic transformations in the Fe-Ni-Cr system.

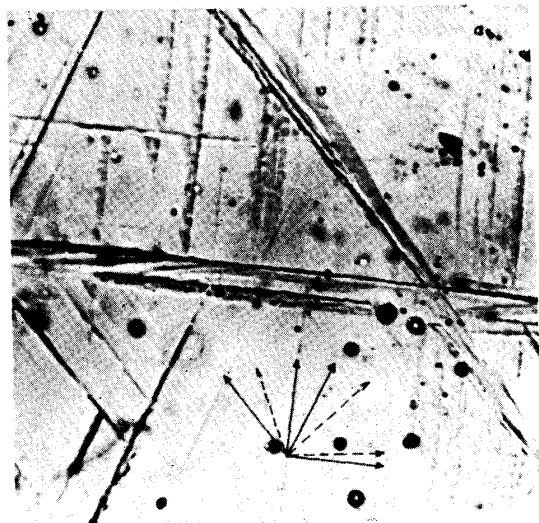


practically change with the increase in Ni content. That is, in Fe-Mn alloy,  $M_s^{\gamma \rightarrow \alpha'}$  point falls rapidly with the increase in Mn content, but  $M_s^{\gamma \rightarrow \varepsilon}$  point gradually. Therefore, it may be assumed that  $M_s^{\gamma \rightarrow \varepsilon}$  point of Fe-Ni-Cr alloy does not practically change so well as that of Fe-Mn alloy. Consequently the point E on the straight line marked EFG in Fig. 4 hardly changes with the change in Ni content, and making the point at which the dotted line passing through the point E and the BHI curve cross each other the point H, then is about 7 per cent Ni. As shown in this figure,  $\gamma \rightarrow \alpha'$  transformation occurs earlier than  $\gamma \rightarrow \varepsilon$  transformation below 7 per cent Ni, whereas above 7 per cent Ni,  $\gamma \rightarrow \varepsilon$  transformation occurs first. The above-mentioned results correspond to the fact that isothermal martensite transformation diagram of Fe-18 per cent Cr alloy containing Ni less than 7 per cent shows the C type curve,<sup>(5)</sup> but that in the case of alloy containing Ni more than 7 per cent T.T.T. diagram of the alloy shows the curve with two noses, as shown in Fig. 2. It is seen from Eq. (1) that the condition for the  $\gamma \rightarrow \varepsilon$  transformation depends on the stacking fault energy.

The relation between  $\varepsilon$  and  $\alpha'$  phases is to be considered crystallographically. In Phot. 1, X-ray diffraction lines of  $\alpha'$  phase are observable together with those of  $\varepsilon$  phase in the specimen which was transformed isothermally at  $-100^\circ\text{C}$ . This shows the fact that  $\gamma \rightarrow \alpha'$  transformation occurs in the temperature range of the upper nose. As shown in Phot. 5,  $\alpha'$  plates in the specimen treated at  $-100^\circ\text{C}$  are formed along the  $\varepsilon$  phase. The habit plane of the  $\alpha'$  plate as well as that of the  $\varepsilon$  phase is  $(111)_\gamma$ . However,  $\alpha'$  plates with another habit plane are also observable. Phot. 6 shows the  $\alpha'$  plates formed while the specimen was held at  $-100^\circ\text{C}$  for about 1 hour. In this photograph, the arrows marked by solid lines and by dotted lines represent  $(111)_\gamma$  traces and directions of  $\alpha'$  plates with unknown habit plane, respectively. Fig. 5 shows the results obtained by one surface analysis. As shown in



Phot. 5.



Phot. 6.

Phot. 5. Microstructure showing  $\varepsilon$  and  $\alpha'$  phases. ( $\times 480$ )

Phot. 6. Microstructure showing four  $(111)_\gamma$  traces and  $\alpha'$  phase. ( $\times 480$ )

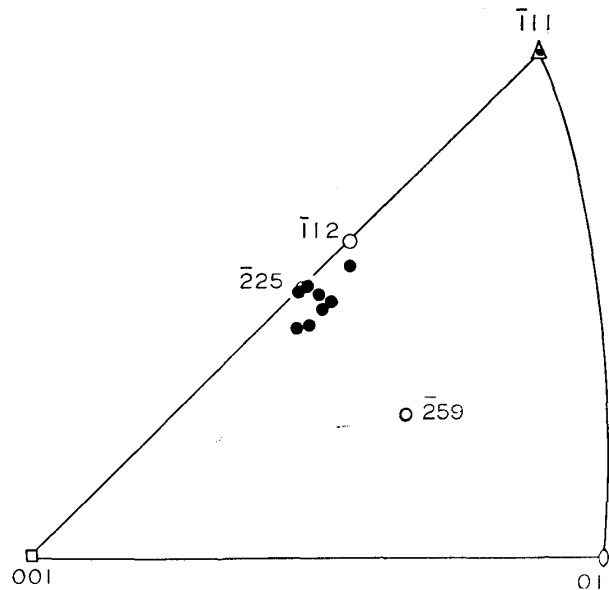


Fig. 5. Martensite habit plane in the Fe-Ni-Cr alloy by stereographic projection. Solid circles represent habit plane.

this figure, the habit planes of these  $\alpha'$  plates are about  $(225)_\gamma$  and agree well with Venable's result<sup>(7)</sup>. It is definitely seen from the above-mentioned results that three kinds of martensites were formed while the specimen was held in the temperature range of the upper nose, that is, the  $\epsilon$  phase having  $(111)_\gamma$  habit plane and  $\alpha'$  phases having  $(111)_\gamma$  and  $(225)_\gamma$  habit planes respectively. On the other hand, three kinds of martensites were also observed while the specimen was held in the temperature range of the lower nose. It is, therefore, conceivable that these plates are formed in the matrix because the specimens pass through the upper nose during sub-atmospheric cooling. If the specimens do not pass through the upper nose, the martensite with the habit plane of  $(225)_\gamma$  only will be observed. It was observed frequently that the tips of  $\alpha'$  plates with the habit plane of  $(225)_\gamma$  were obstructed by the plates with  $(111)_\gamma$  habit plane. This means that the former appears subsequently to the latter. In spite of isothermal holding at  $-100^\circ\text{C}$ , the  $\alpha'$  plates with  $(225)_\gamma$  habit plane are seen in Phot. 6. This will suggest the fact that the  $\alpha'$  plates with  $(225)_\gamma$  habit plane are formed, when the time the specimens are to be held is equal to the incubation time of the lower nose at  $-100^\circ\text{C}$ , subsequently to that of  $(111)_\gamma$  habit plane and the  $\epsilon$  phase are formed at the upper nose. Thus, the  $\alpha'$  plates with  $(111)_\gamma$  habit plane and the  $\epsilon$  phase are formed at the upper nose and the  $\alpha'$  plates with  $(225)_\gamma$  habit plane are formed at the lower nose. The habit plane of the athermal martensite agrees with that of the  $\alpha'$  plate formed at the lower nose and is  $(225)_\gamma$ .

### Summary

An investigation of isothermal martensite transformation was carried out by using 17 per cent Cr-8 per cent Ni-Fe alloy at subatmospheric temperature.

The results obtained are as follows:

(1) Two noses were observed in the isothermal transformation diagram. The  $\varepsilon$  phase was formed at the upper nose and subsequently, the  $\alpha'$  phase having the habit plane of  $(111)_\gamma$  was formed at this nose.

(2) The driving force necessary to initiate the transformation of  $\gamma$  into  $\varepsilon$  phase was derived from an assumption in which a half dislocation could be moved freely, leaving a stacking fault owing to its very low energy, which was 22 cal/mol. It was shown in this treatment that the transformation would occur above 7 per cent Ni content. This result agreed well with practical data.

(3) The habit plane of the  $\alpha'$  formed isothermally in the temperature range of the lower nose and athermally at a temperature below  $M_{\gamma \rightarrow \alpha'}$  was  $(225)_\gamma$  plane.